Chapter 2

The Optical Tweezers

This chapter provides a brief background to the Optical Tweezers, describes some of the applications where Optical Tweezers have been used and reviews the physics required to understand the operating principles of an optical trap. It also describes the equipment and operation of our Optical Tweezers and explains the calibration techniques that are used.

2.1 Background

In 1871 Maxwell [1] theorised that the momentum of light could exert a pressure on a surface, an effect that was later called "radiation pressure". Lebedev [2], and independently, Nichols and Hull [3] experimentally demonstrated that light could exert a pressure on an object in 1901. This pressure was very weak as there was a low photon flux. A large increase in the photon flux was achieved with the invention of the laser in 1960, and with this increase in photon flux it was realised that radiation pressure could be used to perform tasks. In 1971 Ashkin *et al* balanced the radiation pressure exerted by a laser and gravity to trap a 20 μm dielectric particle [4]. Ashkin, among others, continued working in the field of optically trapping particles and published several articles regarding atom and colloidal particle trapping [5, 6, 7, 8]. This work later split into two categories: laser atom cooling and optical trapping. In 1986 Ashkin *et al* [9] reported the first use of a single-beam optical trap to hold particles between 25 nm and 10 μm in diameter at a fixed point in water. Shortly after this publication the apparatus that Ashkin used to trap these particles became known as Optical Tweezers and the method known as optical trapping.

Today Optical Tweezers are used in a variety of ways. In the biological and

medicinal sciences Optical Tweezers are often used to separate different cell types, manipulate sub-cellular objects without damaging the cell itself and for medicinal procedures such as invitro fertilisation. Most commercial Optical Tweezers are aimed at the biological and medical markets and, as such, the wavelength of the lasers in many commercial Optical Tweezers operate in the near infra-red to avoid damaging living cells. But Optical Tweezers are much more useful than a simple sorting and micro-manipulation tool: they can be used for force measurement. By varying the strength of the laser it is possible to exert a force on a particle ranging between 0.001 pN and 100 pN (1 pN = 10^{-12} N). This in turn can be used in single-molecule research [10, 11, 12], for example the stretching of single polymer chains, or to examine the transfer of orbital angular momentum to microscopic particles [13, 14].

New types of Optical Tweezers are also emerging. The latest variant is a set of dynamic holographic optical tweezers, where the trapping characteristics of the laser beam is modified, enabling many more systems to be studied and more applications to be found. Some examples include creating a micro-optomechanic pump [15], optical fractionation [16] and 3D manipulation of particles into crystal structures [17].

2.2 The Physics of Optical Tweezers

This section outlines the basic physics that is required to understand the operation of the Optical Tweezers. This starts by considering the effect of individual photons and concludes by analysing the potential energy landscape generated by the Optical Tweezers.

2.2.1 The Energy and Momenta of Photons

From classical and quantum mechanics it is known that individual photons have energy and momentum [18, 19, 20]. The energy of a photon is given by $E = hc/\lambda$, where E is the energy, h is Planck's constant (6.626×10^{-34}J·s), c is the speed of light in a vacuum and λ is the wavelength of the photon. The corresponding momenta of this photon is $p = h/\lambda$. For example, a photon with a wavelength of 1000 nm has 1.99×10^{-19}J of energy and a momentum of 6.65×10^{-28}N·s. Often

it is convenient to cast energy units in terms of force·distance: pN·nm or pN·μm. The energy of this photon is then 199 pN·nm (0.199 pN·μm). This energy can be compared with several other similar energy terms. For example the hydrolysis of ATP to ADP requires ≈100 pN·nm, an ion moving through an ion channel takes ≈30 pN·nm and thermal energy, k_BT, at room temperature is ≈4 pN·nm. The momentum of a single photon is extremely small and, by itself, has little effect on a nano-sized system. However by using any electromagnetic radiator (for example an LED, microwave, radio transmitter or even a simple light bulb) large quantities of photons can be generated to produce a larger effect.

2.2.2 Interactions of Photons with Objects

A beam of photons can interact with an object in a number of ways. The size of the object is critical to determine the effect of these interactions. Maxwell's equations must be solved to determine how the object will interact with the electric field of the photons when the smallest dimension of the object is smaller than the wavelength of the photons. The review by Padgett *et al* [21] provides further explanation of this scenario.

When an object's smallest dimension is larger than the wavelength of the incoming photons the concepts of reflection, refraction and absorbtion are used. Reflection is determined by the rule: the angle of incidence is equal to the angle of reflection (see Figure 2.1), or more simply, $\theta_r = \theta_1$. Where θ_1 is the angle of incidence from the surface normal and θ_r is the angle of reflection from the surface normal. Snell's law can be used to determine the angle of refraction: $n_1 \sin\theta_1 = n_2 \sin\theta_2$, where n_1 is the refractive index of material 1, n_2 is the refractive index of material 2, θ_1 is the incident angle measured from the surface normal and θ_2 is the angle of the refracted photons, measured from the negative surface normal, as shown in Figure 2.1.

2.2.3 Refraction through a Mie Scattering Particle

Refraction through a Mie scattering particle (a particle whose size is similar or larger than the wavelength of light used to examine it) also imparts momentum perpendicular to the axis of beam propagation. This can be used to show how an optical trap is formed. In the following description two cases need to be considered: $n_p > n_s$ and $n_p < n_s$, where n_p is the refractive index of the particle and n_s is the

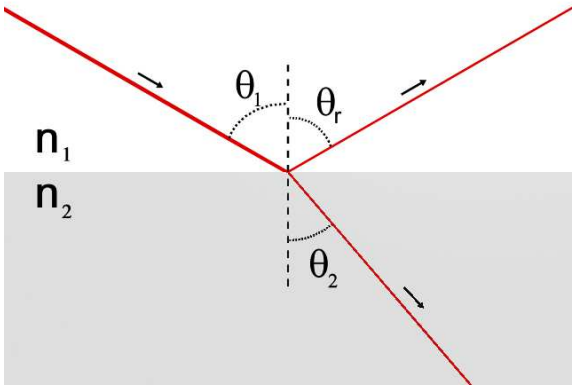

Figure 2.1: An example of refraction and reflection at an interface. The refractive index of material 2 (on the bottom) is larger than the refractive index of the material on top; that is, $n_2 > n_1$.

refractive index of the surrounding medium. I also use the terms used by Ashkin: the axial or scattering forces are forces that act parallel to the direction of the laser beam, and the transverse or dipole forces are forces perpendicular to the laser beams propagation. The terms scattering and dipole are typically used for Rayleigh particles (particles substantially smaller than the wavelength of the incident light) or atoms whereas the terms axial and transverse are typically used for Mie-sized particles.

Figure 2.2 shows the effects of multiple rays being refracted through a microscopic particle. When rays on either side of the particle have the same intensity, Figure 2.2a, the transverse components of the momentum vectors cancel. But if there is an unequal laser intensity on either side of the particle, that is, an intensity gradient is present as indicated by Figure 2.2b, then the particle will move towards (or away) from the most intense region of light. To steer a particle towards a given point, using a particle where $n_p > n_s$, intensity profiles with a strong central peak (for example Gaussian distributions, triangular profiles, etc) draw the particle into the most intense region of the laser beam. If the particle has a lower refractive index than the surrounding media, $n_s > n_p$, or is a reflective particle, a hollow profile is required. Some examples of hollow profiles include profiles with: 2D parabolic, $\cosh\theta$ functional forms and Hermite-Gaussian TEM_{01*} laser modes as shown in Figure 2.3.

Using the laser intensity gradient the particle's position in the transverse plane can be controlled. The final step in creating an optical trap is to control the particle's

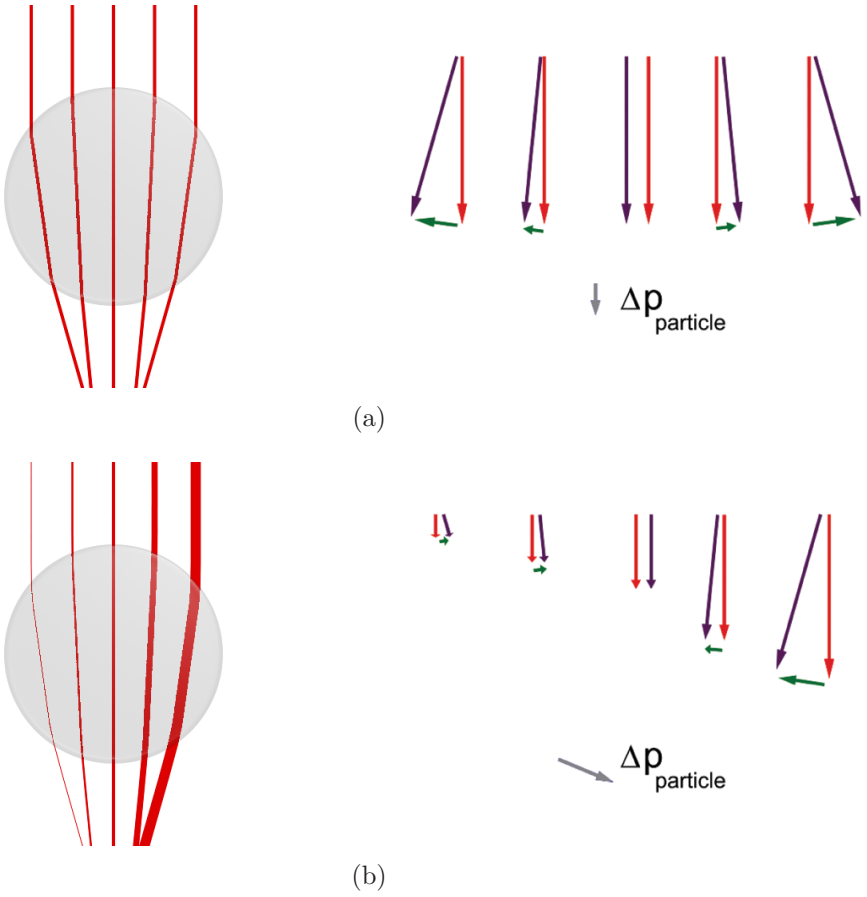

Figure 2.2: Multiple rays are shown as they refract through a microscopic particle. $n_p > n_s$ for both the top and bottom images. The momentum vectors for each of the rays are shown to the right of the particle refraction images. The red vectors represent the incoming momentum, the purple vectors represent the refracted momentum, the green vectors represent the change in momentum, and the grey vector represents the total change in the particle's momentum, $\Delta\mathbf{p}_{\text{particle}}$. (a) Five rays of equal intensity are shown. The resultant vector only acts in the axial direction (in the direction of the beams propagation) after transverse components cancel. (b) Five rays of increasing intensity are refracted through the same particle. Partial cancellation in the transverse axes results, however the resulting momentum vector has components in the transverse and axial directions.

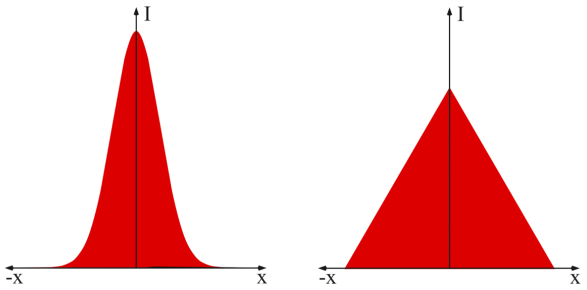

(a) Intensity profiles for when $n_p > n_s$.

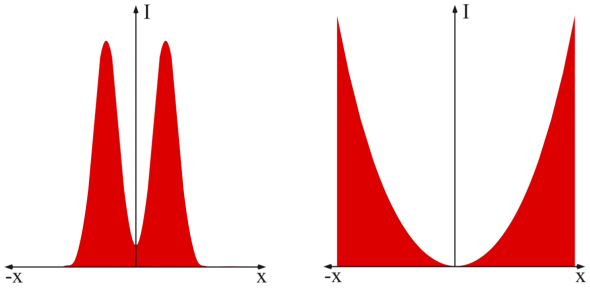

(b) Intensity profiles for when $n_p < n_s$.

Figure 2.3: Shown are some 1D intensity profiles which can be used to hold a microscopic particle. The vertical scale, I, is the intensity while the horizontal scale is distance from a central axis of symmetry. (a) Examples of two profiles that will trap a particle when $n_p > n_s$. (b) Examples of two "hollow profiles" that can be used to help trap a particle when $n_p < n_s$. All of these images should be rotated about their central axis to generate 2D intensity distributions that would be required in a physical system.

position in the axial direction. By inserting a lens into the path of the laser beam an intensity gradient is created along the laser beam's axis. This intensity gradient will again move the particle in the same manner described above: towards the most intense region of light when $n_p > n_s$ and away from the most intense region of light when $n_s > n_p$ as illustrated in Figure 2.4. In addition to creating this axial intensity gradient, the lens effectively increases the intensity gradient in the transverse directions. It is not possible to generate a single beam optical trap for particles whose refractive index is lower than the surrounding solution, $n_s > n_p$. Instead a balance between an outside force (for example an electric field or gravity) and the change in momentum along the laser beams axis is required. This force balance will enable a particle to be trapped above or below the focal point.

A high numerical aperture lens generates a very strong gradient along the axis of beam propagation, and can effectively confine the particle within a focal plane. With such a large intensity gradient thermal fluctuations only have a minor effect on the particle's motion perpendicular to the focal plane, and measurements can be made assuming there is little to no movement perpendicular to the focal plane.

The above concepts form a basic understanding of an optical trap, and how the forces generated by the trap move a particle towards a given point in 3D space. In addition the strength of the optical trap along each axis must be large enough to overcome the forces due to Brownian motion otherwise the particle will "escape" the trap. It should be noted that an optical trap is only formed when a particle is present within the confines of the intensity profile of the laser beam, otherwise the system is simply a focussed laser beam.

2.2.4 Reflection from a Mie Particle

The forces that act on a reflective particle operate in a similar manner to the forces generated when the refractive index of the solvent is larger than that of the particle, $n_s > n_p$. The momentum transferred to the particle in the transverse directions moves it away from the most intense region of the laser beam and a balance between an external force and radiation pressure must be used to create the optical trap. An example of a reflective optical trap is shown in Figure 2.5. Localised heating may also occur in these reflective solutions, which may cause other effects within the solution such as localised fluid flows. Reflective particles are generally used in Magnetic

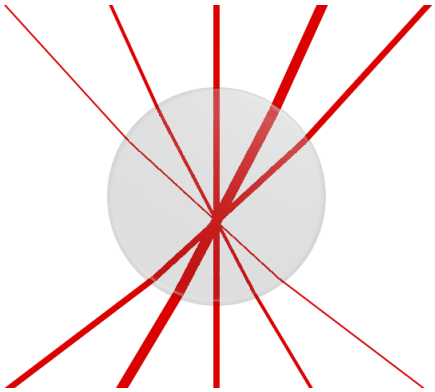

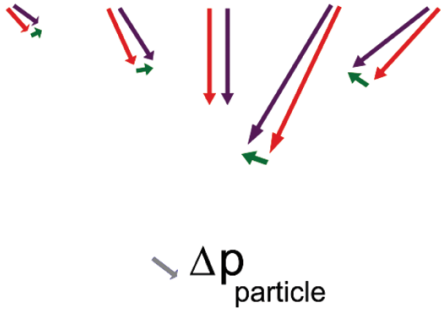

(a) $n_p > n_s$

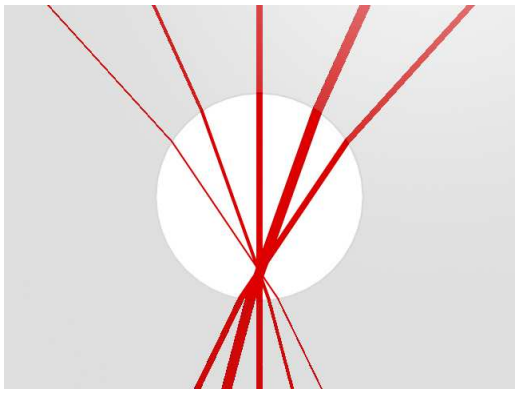

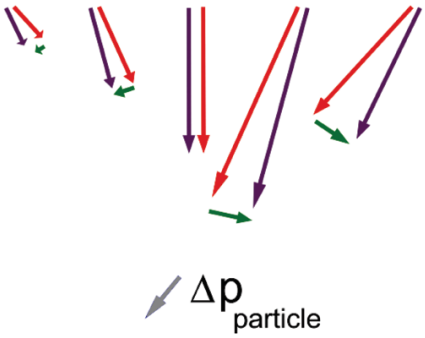

(b) $n_s > n_p$

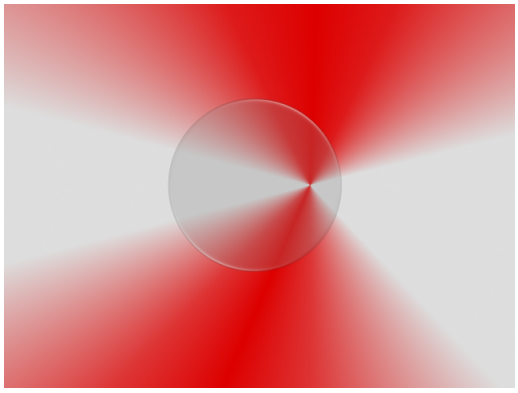

(c) $n_p > n_s$ - continuous view

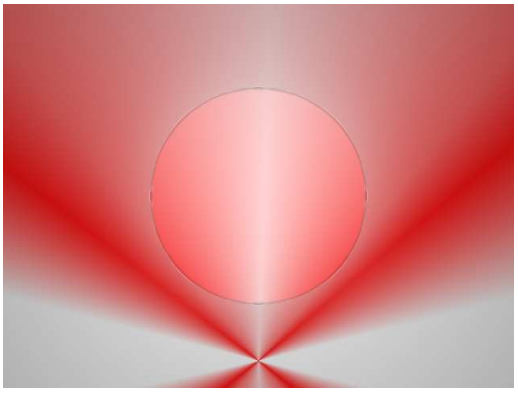

(d) $n_s > n_p$ - continuous view

Figure 2.4: By using a lens to focus the laser beam a point is created that the particle tries to restore itself to or move away from. The red vectors represent the incoming momentum, the purple vectors represent the refracted momentum, the green vectors represent the change in momentum, and the grey vector represents the total change in the particle's momentum, $\Delta \mathbf{p}_{\text{particle}}$. (a) The ray diagram for $n_p > n_s$. (b) The ray digram for $n_s > n_p$. (c) An example of a continuous view for $n_p > n_s$. Higher light intensities are illustrated using darker red colours. (d) An example of an intensity profile with a low central intensity for $n_s > n_p$. A force balance is required to maintain the particle's position at a given coordinate.

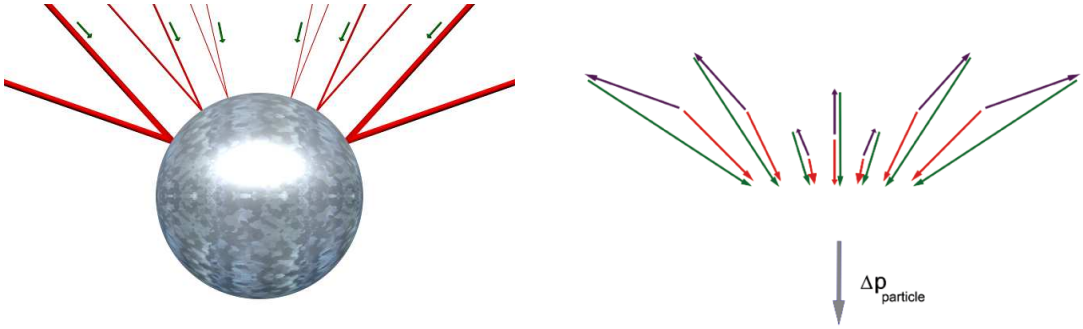

Figure 2.5: An optical trap that uses reflection to trap a particle. The red vectors represent the momentum of incoming photons, the purple vectors represent the momentum vectors of reflected photons, the green vectors represent the change in momentum, and the grey vector represents the total change in the particle's momentum, $\Delta \mathbf{p}_{\text{particle}}$ which must be balanced by an external field.

Tweezers rather than Optical Tweezers or when high localised temperatures are required.

2.2.5 Photon Flux

An example is given below to determine the number of photons required to manipulate a microscopic particle. The parameters and description that follows are meant only as a rough guide, several minor effects are not included.

Consider a microscopic sphere, 10 μm in diameter, that is moved at 1 μm·s^{-1} through a fluid (water) with a viscosity of $\eta = 1.0 \times 10^{-3}$ using photons with a wavelength of 1000 nm. The energy of each photon is 1.99×10^{-19} J and the momentum of each photon is 6.65×10^{-28} N·m. The surface area of the sphere is calculated to be 3.14×10^{-10} m^2. Using Stokes' drag, $F_{drag} = 6\pi\eta aV$ the force required to achieve this is 1.885×10^{-13} N, where a is the radius of the sphere. Therefore dividing F_{drag} by the momentum per photon shows that 2.8345×10^{14} photons hit the surface perpendicularly per second to maintain this velocity, assuming that every photon is absorbed by the particle. Calculating the power per unit area this corresponds to 17.95 W·cm^{-2}, or approximately 180 times the power flux of ordinary sunlight. The most common type of photon emitter capable of producing such an intense focussed beam is the laser.

If reflection is considered instead of absorption then the average change in mo-

mentum imparted to the sphere is ≈1.525 times larger[1] than that acquired by absorption. However in the case of refraction the average change in momentum is significantly lower. For example, if $n_1 = 1.33$ (water) and $n_2 = 1.55$ (polystyrene) then the average change in momentum imparted to the bead is only 0.0389 times that of absorption[2]. As the relative ratio of the refractive indices increases, $\frac{n_2}{n_1}$, there is a corresponding increase in the momentum change, although it is still only a small fraction of the momentum transfer possible with absorption. The momentum imparted to the particle moves it along the axis of beam propagation.

2.2.6 The Optical Tweezers as a Potential Well

Many experiments and calibrations [21, 22] have shown that the radiation pressure exerts a Hookian restoring force on a particle when it is located within the focal plane and its position is located near the focal point. That is $\mathbf{F} = -k\mathbf{r}$ where $\mathbf{F}$ is an optical force that acts on the particle within the focal plane, k is the trap or spring constant and $\mathbf{r}$ is the displacement of the particle from the laser beam's focal point. The potential energy, U, is simply: $U = \frac{1}{2}k\mathbf{r} \cdot \mathbf{r}$. Figure 2.6 shows two illustrations of potential wells with different trap constants.

Figure 2.6 illustrates how the energy of the system changes as the trap strength is increased. The yellow ring represents thermal energy, k_BT and the particle will reside below this energy if no external forces are acting on the particle. The particle in the weak trap, Figure 2.6a, is able to sample a larger region than the particle in the strong trap, Figure 2.6b. This has implications in the design of experiments that test the Fluctuation Theorem in later chapters of this thesis.

2.3 Instrumentation

In general, Optical Tweezers integrate several pieces of equipment to generate and control an optical trap. The Optical Tweezers used in this thesis differ significantly from most commercially available sets of Optical Tweezers as several modifications have changed the apparatus from a biological separation tool to an accurate force measurement device. These changes have enabled us to measure the forces gen-

[1] This was calculated numerically by reflecting 5000 rays off a particle, setting the laser beam width equal to the particle's diameter and assuming a uniform intensity.

[2] This was calculated numerically by refracting 5000 rays through a particle, setting the laser beam width equal to the particle's diameter and assuming a uniform intensity.

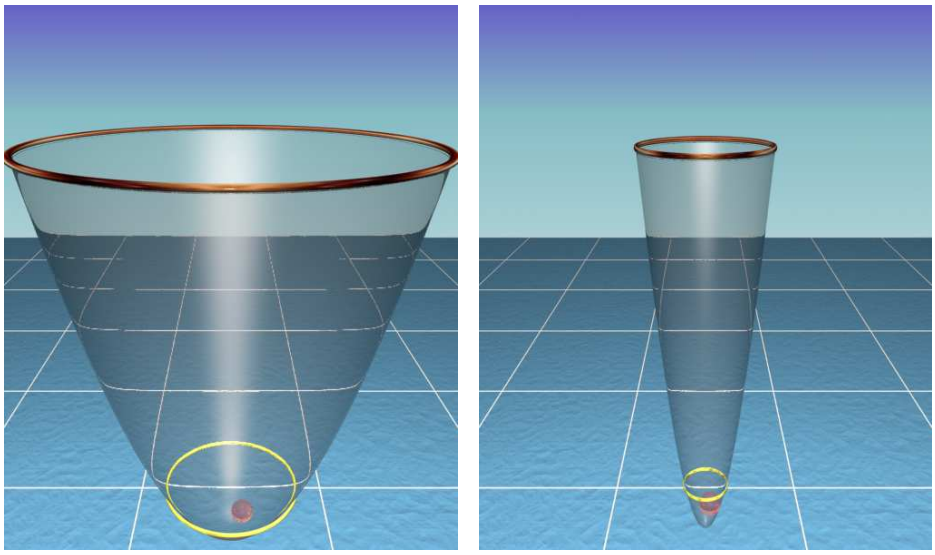

(a) (b)

Figure 2.6: Two Optical Tweezers potential wells. In these figures the vertical axis represents the potential energy, U, and the grid represents the distance from the center of the optical trap (located at the bottom of each potential well). The yellow ring in both figures represents thermal energy, or $U = k_B T$. Without any other external forces, other than the optical trap and thermal motion, the particle is expected to be located below the thermal energy ring. (a) The particle in a potential well with a weak trap constant, k. (b) The particle in a potential well with a strong trap constant.

erated by the optical trap and enabled better control of several Optical Tweezers components. This section describes the original, commercially available version of the Optical Tweezers and the modifications our research group has made to the device.

2.3.1 The Original, Commercial Setup

The original version of the Optical Tweezers (Cell Robotics Inc., USA) was sold as a device that could separate biological cells and other transparent particulates - it had no force measurement capabilities. This set of Optical Tweezers consisted of the following components:

- an inverted microscope,
- a stepper motor controlled microscope stage,
- a CCD camera,
- a micro-fluidic delivery device,
- an infra-red laser,
- and a computer to control the components.

A Nikon DIAPHOT 300 inverted microscope is used as a basic framework to integrate other components into the system. The microscope is fitted with 4 oil-immersion objective lenses: 40×, 60× and two 100× with numerical apertures of: 1.3, 1.4, 1.3 and 1.4 respectively and one standard 10× objective with a numerical aperture of 0.3. It should be noted that an optical trap cannot be established for the 10× lens as the numerical aperture is too low - that is, the laser beams intensity gradient along the axial direction is not large enough to trap a micron-sized particle at its focal point. In contrast the high numerical aperture lenses provide a very large gradient along the axis of beam propagation, enabling the particle to be effectively captured within the focal plane. This setup does not allow measurements of displacements along the axis of beam propagation; however this can be qualitatively judged by examining the image of the trapped particle.

The microscope stage has two servomotor-controlled micrometers acting in orthogonal directions. Each micrometer is capable of moving ±10 mm with an accu-

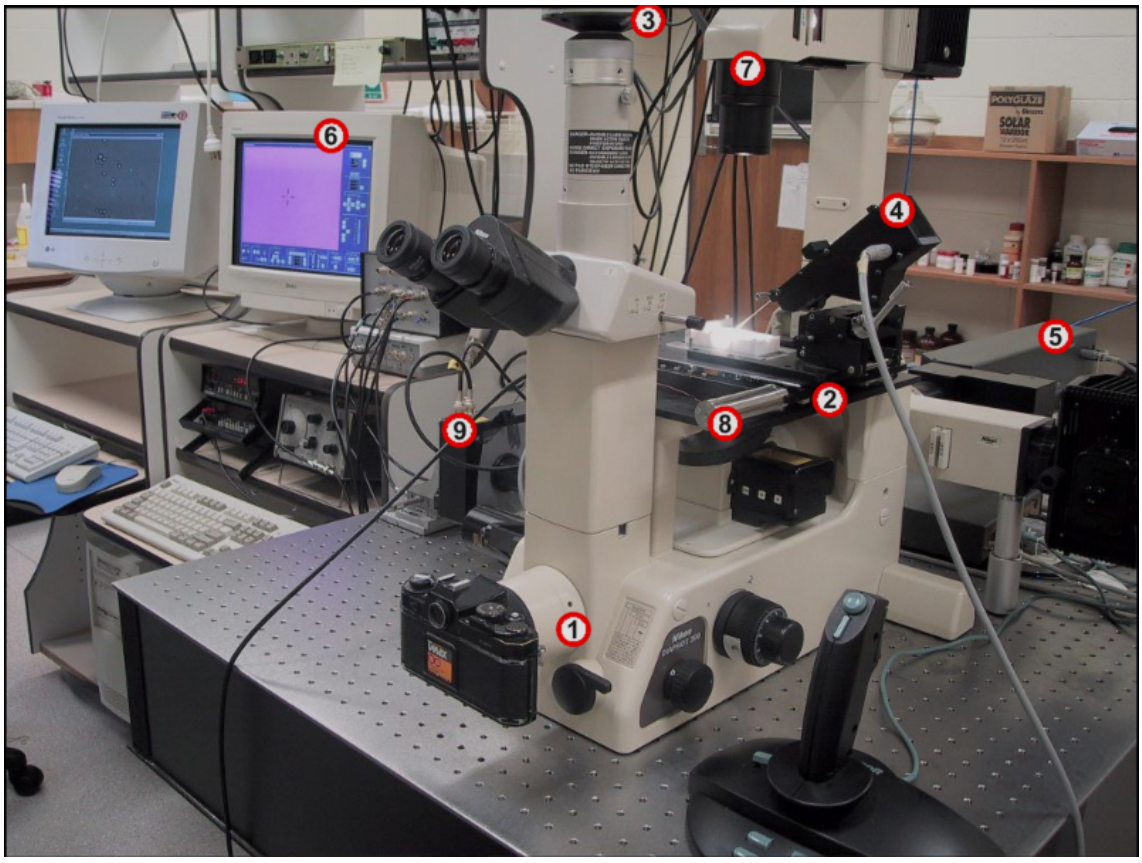

Figure 2.7: The photo shown was taken in June 2002, before most major modifications were made to the system. The numbered components correspond to the following: (1) Nikon Diaphot 300 inverted microscope, (2) Microscope stage, (3) MTI IFG CCD Camera, (4) Microfluidic delivery device, (5) Cell Robotics Laser, (6) Original control computer (7) light source, (8 - above) open loop piezoelectric translator, (8 below) microscope objectives, (9) quadrant photodiode position detection system, built in-house. Components (8) and (9) are additions to the original, commercial set-up.

racy of 0.1 μm, but is limited to ± 8 mm in the x-direction and ± 5 mm along the y-axis. The maximum controllable velocity is 200 μm$\cdot$s^{-1}.

The MTI IFG 300 CCD camera is used to visualise the system. The camera is mounted on the ocular column of the microscope and projects images of the system to the computer at a rate of 25 frames per second (film speed). The resolution is 5.8 pixels/μm using a 100$\times$ lens.

An infra-red laser (Cell Robotics, USA) is fitted to the rear port of the microscope and has a wavelength of $\lambda = 985 \pm 5$ nm. The laser has a variable power input, enabling the laser power output to be changed in integer steps from 1% power to 99%. By varying the output power of the laser the strength of the optical trap is modified. As the laser beams intensity profile is not a TEM_{00} mode, the x and y trap constants are not symmetric. However, at low laser power the trap constants in the x and y directions are approximately equal, allowing us to treat the trap as symmetric. The CCD camera, laser power, objective focus and servomotors were all controlled by a dedicated computer through interfaces developed by Cell Robotics Inc. USA.

2.3.2 Trap Asymmetry

A side effect of the original commercial set-up is that the laser beam exhibits properties indicative of single slit diffraction. It is also possible that there are several different laser modes interfering with one another producing a similar result, however the sealed laser cavity prevents us from correcting the problem. Figure 2.8 shows a photo of the laser beam, taken through an IR viewer.

This non-uniform distribution of beam intensity has many advantages for a biologist wishing to sort different cell types. For example it enables cylindrical objects to align themselves with a predefined orientation within the trap. However, as there is not a uniform photon flux, difficulties arise with force measurement as the trap constant may vary depending on its orientation. When there is trap asymmetry different trap constants are obtained by rotating the detector around the axis of beam propagation. In comparison, a correctly aligned 2D-gaussian TEM_{00} beam has equal trap constants in all directions regardless of whether it is rotated or not.

It is also common practice with Optical Tweezers to overfill the rear aperture of the trapping lens with the incoming laser beam. That is, not all of the laser

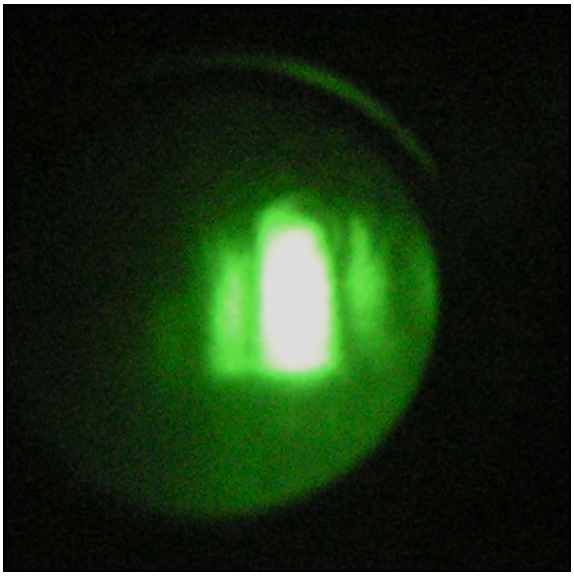

Figure 2.8: A photo of the NIR laser spot supplied by Cell Robotics viewed through an infra-red viewer. The fact the laser spot does not have a gaussian intensity distribution means that obtaining equal trap constants along both the x and y axes is very difficult.

beam is passed through the final lens, thereby enabling visual alignment of the laser beam before fine-tuning the intensity at the output. By using only the most central and intense part of the laser beam many problems due to interference can be eliminated and a pseudo-symmetric optical trap may be obtained. This is verified by performing several equipartition calibrations (Section 2.5.4) on various particles and checking to ensure that the calculated trap constants along both the x and y axes are approximately equal. Should they not be equal, the laser beam should be re-adjusted and the equipartition process repeated until the constants are approximately equal over the desired laser power range.

2.3.3 Modifications to the Optical Tweezers

Various components have been added to the Optical Tweezers to enable accurate force measurement and allow automation. The equipment acquired includes:

- a quadrant photodiode to enable force measurement,
- a second computer to monitor the image acquisition (CCD camera) independently of the control software,
- a replacement control computer with Labview software (National Instruments, LabView v7.1, USA) to automate various functions and replace the original

control software,

- a data aquisition card (National Instruments, PCI NI-6014, USA),
- two open-loop piezo translators,
- two closed-loop piezo translators (Physik Instrumente, P-814.40, Germany),
- an arbitrary function generator (Thurlby Thander Industries, TGA 1242, UK),
- a DAGE image intensifier (MTI IFG 300, USA),
- and a laser stabliser (BEOC, LPC-NIR, USA).

The most important modification to the Optical Tweezers is the addition of the quadrant photodiode, shown in Figure 2.9. This addition enables the Optical Tweezers to measure the displacement of a particle from the focal point of the laser to within 15 nm using a 100× lens. After calibrating the quadrant photodiode system the position of the particle can be recorded and the forces acting on the particle can be calculated. The 3×3 mm quadrant photodiode (Hamamatsu, S4349, Japan) is located through the side port of the microscope and is illuminated by an image of the particle. The particle's image produces a voltage in each quadrant of the photodiode. Using an amplifying electronic circuit, with addition and subtraction of voltages, the individual photodiode quadrant signals are converted into a voltage in both the horizontal and vertical directions. After a photodiode calibration has been performed (see Section 2.5.2) these voltages can be used to measure the displacement of the particle from the center of the optical trap.

A second computer has been purchased specifically to view and/or record the images produced by the CCD camera (P3 666MHz, 256MB RAM, 40Gb SCSI HDD). This second computer ensures that the original computer is always able to control the Optical Tweezers and record voltages using a data acquisition card (DAQ), and vice versa. In conjunction with the DAQ of the control computer, this computer allowed us to save images and the corresponding voltage signals in parallel.

A third computer (P4 2.4GHz, 512MB RAM, 80Gb HDD) was purchased with Labview software (National Instruments, LabView v7.1, USA) and a new data acquisition card (National Instruments, PCI-6014, USA). The new data acquisition card (DAQ) was required as computer architecture has changed dramatically since the original DAQ was purchased. The NI DAQ is able to record a wider range of

voltages, record data at higher sampling rates (up to 200,000 Samples/s) and has better accuracy with 16 signal bits as opposed to 12. Using Labview I have written programs to control and automate the optical tweezers and DAQ. These programs have enabled us to replace the original control computer and software, providing a more flexible system in which to operate.

Originally two open loop piezo translators were purchased, fitted to the x and y axes of the stage, enabling fine stage displacements to occur. When a voltage is applied to these open loop piezo crystals they expanded up to 60 μm. However the open-loop control system provided no feedback controls to verify that the input signal corresponds to the output translation. Testing revealed that the piezo translators operated in a non-uniform, non-linear manner and that the zero point suffers from piezoelectric drift. To overcome these deficiencies two new, closed-loop piezo translators were purchased. These piezo translators use strain gauges to provide feedback, ensuring that the piezo extends the required distance, eliminating hysteresis and zero point drift. It is claimed that these piezo crystals are accurate to within 1.2 nm, which is better than our detectors resolution. Testing has shown that the movement is indeed linear within our detection range. In addition new housing units were designed to protect the piezo translators and to enable them to be fitted to the microscope stage.

The arbitrary waveform generator (Thurlby Thander Instruments, TGA1242, UK) can output any electrical voltage ranging from -10V to 10V. It operates at frequencies ranging from 1mHz to 40MHz. The waveforms are converted from a 12 bit digital signal to an analog voltage, with an accuracy of ± 1 bit (or $2.4 \times 10^{-4} \times V_{p-p}$, where V_{p-p} is the input peak to peak voltage). The arbitrary waveform generator can also output all the functions available on a standard function generator. This arbitrary waveform generator is used to control several different functions, depending on the experiment being carried out. It can be used as a driving signal to move the stage along any 2-dimensional path and to supply the control signals required to automate the Optical Tweezers.

A photodiode (Honeywell, SDP86001, USA) is located above the sample cell and is used to verify when the laser intensity is increased. This photodiode is not used for quantitative data collection, but rather as a qualitative guide to the laser beam's intensity.

Several outside factors can affect the output of the laser, such as the laser temperature and the mains power loading. The laser stabiliser is used to ensure that there is no drift in laser power over a period of time. An internal feedback mechanism, operating at 5kHz, dynamically adjusts a transmission LCD to maintain a constant laser output (to within 0.05%). However the stabiliser takes a significant time (between 2 and 70 ms) to reduce its power, especially when large changes are made to the laser power. As such the stabiliser should only be used when the decrease in the power of the optical trapping constant does not occur too rapidly.

The original laser failed in early-mid 2004 requiring a new laser to be purchased. A 4W, $\lambda = 1064$ nm NIR laser with TEM_{00} output was purchased (Compass-4000M, Coherent Scientific, Australia). The laser has a feedback mechanism that checks the power of the laser to ensure that the output power corresponds to the setpoint power. A wider range of laser powers are accessible than the original Cell Robotics laser and the TEM_{00} mode (with correct alignment) overcomes the problem of producing asymmetric traps.

The fully modified Optical Tweezers can be viewed in Figure 2.9. By comparing with Figure 2.7 it is clear that many changes have been made to the system and with much of the original equipment being replaced.

2.3.4 The Quadrant Photodiode System in Detail

Before the exact details of the quadrant photodiode can be discussed the optical path needs to be described. Figure 2.10 illustrates the fundamental visible light path used in our system. The light source is used to illuminate our system and an image of the system is projected into the microscope objective. This image is then passed through a beam splitter and 90% of the light is used to project an image of the system onto the quadrant photodiode, the remaining 10% is used for the CCD camera. As the light source is very weak after passing through the 100× magnification lens the quadrant photodiode signals are passed through a 2-stage amplifying circuit before being sampled by our DAQ card. While the 2-stage amplification reduces the signal to noise ratio (as does any additional electronics) the amplification reduces the relative amount of interference from other signal sources (such as interference from mains power) and raises the signal voltages to ranges that are suited for our DAQ. The amplifying circuits were designed within the school by

Figure 2.9: This photo was taken in June 2005, after the system was significantly modified. The components in the photo are: (1) Nikon Diaphot 300 inverted microscope, (2) Microscope objectives, (3) Microscope stage, (4) Coherrent Compass 4000M Laser, (5) BEOC Laser Stabiliser, (6) MTI IFG CCD Camera, (7) Physik Instrumente Piezo Translator, (8) replacement control computer with custom written Labview software, (9) Sample Cell built in-house.

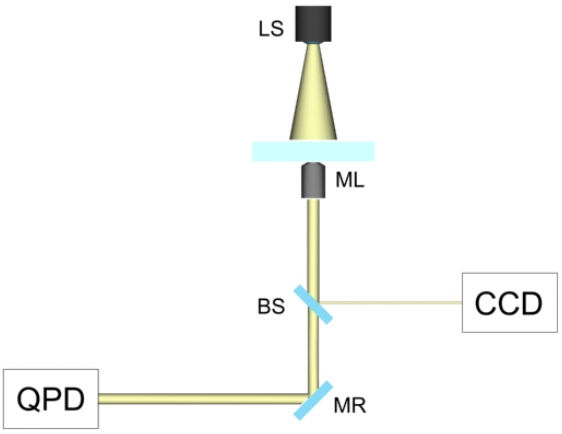

Figure 2.10: An illustration showing how the light progresses from its source (LS), passes through the sample and a microscope lens (ML) before being split 10%/90% at a beam splitter (BS). 10% of the light is delivered to the CCD with the remaining 90% being reflected off a mirror (MR) and passed to the quadrant photodiode position detector.

Dr. Liam Waldron and Russell Koehne.

The quadrant photodiode has four independent photodiodes arranged in a 2×2 array. The signals from the four quadrants are added together electronically using the following equations to give horizontal and vertical voltages, V_H and V_V.

$$V_V = (Q_1 + Q_2) - (Q_3 + Q_4) \tag{2.1}$$

$$V_H = (Q_1 + Q_4) - (Q_2 + Q_3) \tag{2.2}$$

where V_H is the output voltage for the horizontal displacement, V_V is the output voltage for the vertical displacement, and Q_x is the voltage produced in quadrant x. Figure 2.11 illustrates the location of the four quadrants of the photodiode. When calibrated these signals accurately reflect the position of a particle.

The resolution of the photodiode is directly related to the magnification of the particle's image. In general, the higher the magnification the higher the accuracy of the photodiode's signals. However, two factors need to be considered when determining the amount of magnification to use: the photon flux striking the quadrant photodiode and the measurement range. Firstly, a minimum photon flux is required to activate the individual elements within each quadrant of the photodiode. If this flux is not achieved then the signal obtained is dominated by the photodiode's dark current. This scenario can occur if the image of the particle is magnified too much

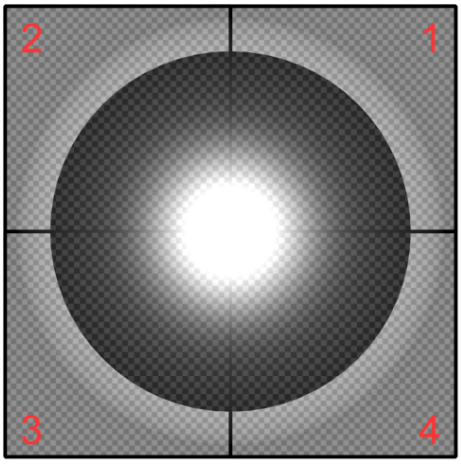

Figure 2.11: A quadrant photodiode is shown with the various quadrants labelled as marked. The quadrant photodiode is illuminated by an image of the particle as shown and the relative contributions to the voltage measured.

as the intensity, I, is related to the field of view, R, in an inverse square manner; that is $I \propto \frac{1}{R^2}$. Additionally, when amplifying the voltage signal, the bandwidth of the device is reduced preventing high frequencies from being recorded. The whole system has a maximum bandwidth of 1 kHz. Secondly, the image of the particle fills most of the active area on the photodiode as indicated in Figure 2.11. Further magnification results in the particle's movements occurring outside the detection range of the photodiode.

The signal generated by the quadrant photodiode depends directly on the image of the particle. Figure 2.2, page 9, shows that parallel rays of light are concentrated as they refract through a particle (assuming $n_p > n_s$). If an imaging plane is inserted somewhere after the particle then it is possible to obtain the images shown in Figure 2.12. The dark regions in these images correspond to areas where the light has been refracted through the particle, and consequently there is little to no photon flux. These additional photons contribute to the bright central core before diverging. When this knowledge is applied to the photodiode one realises that the photodiode measures the following quantity:

$$Q_x = (V_{BG} - V_{Dark}) + V_{Bright} \tag{2.3}$$

where Q_x is the voltage in one quadrant of the photodiode, V_{BG} is the voltage

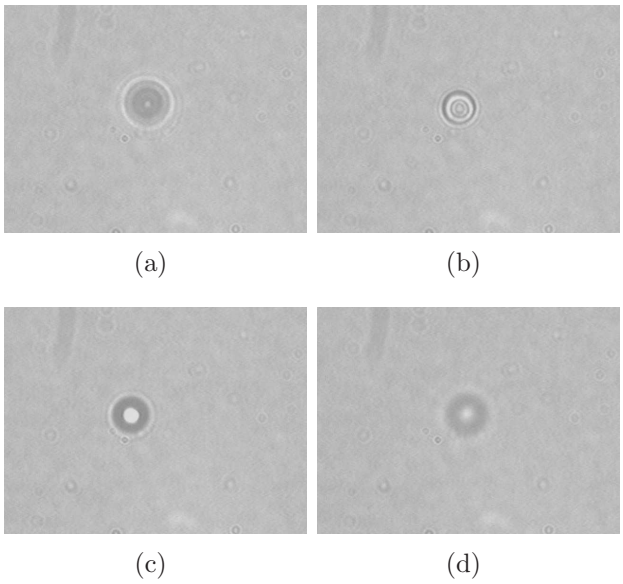

Figure 2.12: Photos of a particle at various heights in the solution are shown. (a) The particle when it is significantly below the focal plane. (b) The particle is located just below the focal plane. (c) The particle has moved into an active optical trap and is held within the focal plane. (d) The particle when it is located above the focal plane.

of the background light source alone acting over the entire quadrant, V_{Dark} is the voltage that an opaque particle would project on the quadrant, and V_{Bright} is the voltage of the central bright spot from the refraction through the particle. Using this model a series of calculations can be constructed to determine the voltage in the horizontal or vertical direction, V_H and V_V in Eqn 2.2, as a function of the particle's position. Figure 2.13 shows that the calculated voltages are similar to those determined experimentally.

2.4 Optical Trapping and Simple Operation of the Optical Tweezers

This section briefly outlines some simple functions of the Optical Tweezers, the equipment required to perform these tasks and some standard methods to trap and move particles. Many of the functions are incorporated in the new LabView control software.

The stage of the Optical Tweezers can be moved using the control software. The user simply selects the maximum speed to move at and, while holding down a mouse button, drags the cursor to somewhere else on the display. This sends a

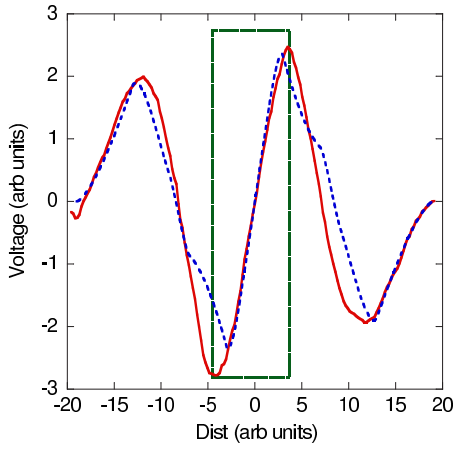

Figure 2.13: A comparison between the position-voltage curve of the quadrant photodiode for the model system proposed in Eqn 2.3 and an experimentally determined curve. The model's curve is shown as (– – –) and the experimental curve is shown as (—). The data contained within the boxed section provides a unique solution when converting voltage to position and represents the photodiode's detection range.

signal to the servomotor-controlled micrometers to move the stage in the selected x-y direction at the given speed. Coordinates can be stored so that the Optical Tweezers can investigate a different section of the sample cell and later return to the stored location. The control software also allows the laser to be switched on and off, and the laser's output power can be modified. Furthermore the laser power stabiliser can be accesed from the software to set the desired power for constant power operation or the maximum power when modulating the laser power.

Using the control software and the 10× lens the sample cell is scanned for particles that can be optically trapped. The lens is changed when a desired particle is located (typically to the 100× N.A. 1.3 lens), the laser is switched on and the particle moves into the focal plane. This is indicated by the particle changing focus when it is not in the focal plane, or by changing its position. To ensure the particle is trapped the stage is translated slowly, which effectively applies a fluid flow relative to the trap. Provided that the particle remains near the focal point during the translation over 10's of microns then the particle is considered to be trapped. Figure 2.12 shows the particle at various times before and after the particle has been trapped. If the particle is below the focal plane when the laser is switched on then Figures 2.12a-c result as the particle moves into the optical trap. If the particle is slightly above the optical trap then it proceeds via the route shown in going from Figure 2.12d to 2.12c.

The arbitrary function generator and the piezoelectric translators can be used to move the stage along a predefined 2D pattern. Any 2D pattern can be followed provided the hydrodynamic drag force isn't larger than the optical trapping force, otherwise the particle will exit the optical trap. The arbitrary function generator can be used with the laser stabiliser to modulate the laser power in a predetermined manner, and hence change the optical trapping constant k. Microfluidic flow fields can be achieved by translating the stage at a set velocity, by using the syringe pump to inject/withdraw fluid at a specific rate or both.

2.5 Calibration of the Optical Tweezers

To ensure that experimental results obtained from the Optical Tweezers are correct each piece of equipment needs to be calibrated before it is used. Some calibrations only need to be performed once, others need to be performed before every experiment, and many of the calibrations are directly dependent upon quantities calculated from previous calibrations. For example, in order to determine the quadrant photodiode calibration it is first necessary to know the amount of magnification that occurs between the input lens and the photodiode. Similarly, to determine the strength of the optical trap (that is, the optical trapping constant k) it is first necessary to know the calibration curve of the quadrant photodiode. The most fundamental calibrations are presented first, followed by the dependant calibrations.

2.5.1 Optics Calibration

The most fundamental quantities in our system are the magnification factors generated by the optics within the system. All other calibrations in the system require accurate knowledge of these magnification factors. For this reason careful analysis of the optical path is required. The technique for obtaining each magnification factor is presented below.

Screen-Size Magnification

The image of the system that is projected onto the CCD camera, and consequently displayed on the computer, is used in several analysis programs. The screen magnification, M_S, is found by placing a standardised ruler with 10 μm increments on the

Optical Tweezers stage and bringing it to a sharp focus. The maximum number of increments shown on the screen is measured, D_S, and compared to the known size, D_A. The magnification was determined using the relation

$$M_S = \frac{D_S}{D_A}. \tag{2.4}$$

Using this relation, pictures recorded by the CCD camera can then be analysed to determine the actual size of image features. M_S is a constant for each lens. Furthermore it is possible to determine the resolution as the CCD can only project at most 768×576 pixels. By dividing D_S by the number of pixels, N_P, required to show the image of D_A on the screen it is possible to determine the size of each pixel, D_P. Using $D_P = D_A/N_P$ the size of each pixel can be calculated, for example when using the 100× N.A. 1.3 lens each pixel has an area of 175×175 nm.

Magnification at Photodiode

To accurately measure the forces acting on a particle it is essential to know the magnification at the quadrant photodiode, M_P. A standardised ruler with 10 μm increments is placed on the Optical Tweezers stage and brought to a sharp focus. An imaging plane is inserted at the quadrant photodiode and the separation between several increments is measured. The separation, D_P, is compared to the actual size, D_A, and the magnification is calculated using

$$M_P = \frac{D_P}{D_A}. \tag{2.5}$$

M_P is also a constant for each individual lens. From the previous two calibrations it is possible to determine the magnification that occurs between the CCD camera and the photodiode, M_{SP}. This is a constant for the entire system as the effect of differing microscope lenses cancels. It is found by

$$M_{SP} = \frac{D_S}{D_P} \tag{2.6}$$

The values found from these calibrations are shown in Table 2.1.

There is also a magnification that occurs between the side port of the microscope and the photodiode. By inserting the imaging plane at various distances from the side port it is possible to determine the relationship between the location of the

Lens	M_S	M_P	M_{SP}
10x N.A. 0.30	164.3	44.5	3.692
40x N.A. 1.30	658	171.4	3.839
60x N.A. 1.40	970	275	3.527
100x N.A. 1.30	1600	400	4.000

Table 2.1: Magnification factors for the various lenses. The values M_S and M_P depend upon the relative set-up and are correct at a fixed distance of the photodiode from the apparatus.

quadrant photodiode and the imaging planes distance, although this not necessary as the quadrant photodiode is a set distance from the side port. The values in Table 2.1 are recorded at a fixed location 150 mm from the side aperture of the Optical Tweezers, at the quadrant photodiode.

2.5.2 Quadrant Photodiode Calibration

As has been described in Section 2.3.4, the quadrant photodiode and amplifying circuit detects the position of a particle that moves within the focal plane. A series of voltages are produced in each quadrant and, following addition and subtraction, horizontal and vertical voltages can be determined. But as the quadrant photodiode is very sensitive to the size of a particle, and the corresponding change in light intensity and pattern, this calibration needs to be performed each and every time a different particle is held in the trap if forces are to be measured. Other factors can also affect the transmitted light, including the constitution of the solution, the variability in particle size, the thickness of the lens oil and the illuminating light's intensity.

The quadrant photodiode is calibrated using the following procedure.

i. A particle is trapped in the Optical Tweezers at high laser power and its image is projected onto the quadrant photodiode. At high laser power the particle's Brownian motion is confined to an area smaller than the resolution of the detector, effectively immobilising the particle; that is, the particle has no fluctuations in its position.

ii. The position of the quadrant photodiode housing is precisely translated using micrometers so that a signal approximately averaging 0 V is obtained along both the horizontal and vertical axes, corresponding to the Optical Tweezers

y and x axes respectively.

iii. The photodiode is translated until the minimum signal is obtained along one axis, no change should occur to the signal on the perpendicular axis. This moves the location of the photodiode relative to the particle's image.

iv. Using the micrometer the photodiode is moved incrementally in 0.04 mm steps and the voltage profile is recorded. This displacement corresponds to moving the photodiode 0.04 mm relative to the *magnified* image of a "stationary" particle, that is distances of 0.04 mm $\times M_P$. The relative photodiode position is consequently converted into an effective particle position by dividing by the magnification factor. A different voltage is recorded for each increment in position.

v. The effective displacement of the particle is plotted against time to produce a graph with a series of "steps", see Figure 2.14. The duration of each "step" is not important, only its voltage. The average voltage for each step is calculated and plotted against relative position, Figure 2.14 inset. A 3rd order polynomial is fitted to the points which is then used to convert the quadrant photodiode's output voltage to the position of the particle within the trap.

vi. The quadrant photodiode is returned to its zero position and the procedure is repeated along the other axis.

The electronic noise due to the background image determines the resolution of the detector. To measure the electronic noise an image of the background (uniform illumination with no particle) is projected onto the quadrant photodiode and the resulting voltage waveforms are measured. This waveform is typical of gaussian white noise. Using an arbitrary particle's quadrant photodiode calibration curve enables the effective positions of a hypothetical particle to be calculated. The resulting spread of values corresponds to our claimed ± 15 nm resolution. An alternate method is to repeat the quadrant photodiode detectors calibration using a particle that is stuck to the bottom of the sample cell. After returning the detector to zero, a series of voltages are recorded and these are converted to displacement. Again a gaussian spread of values is generated with a distribution of approximately ± 15 nm.

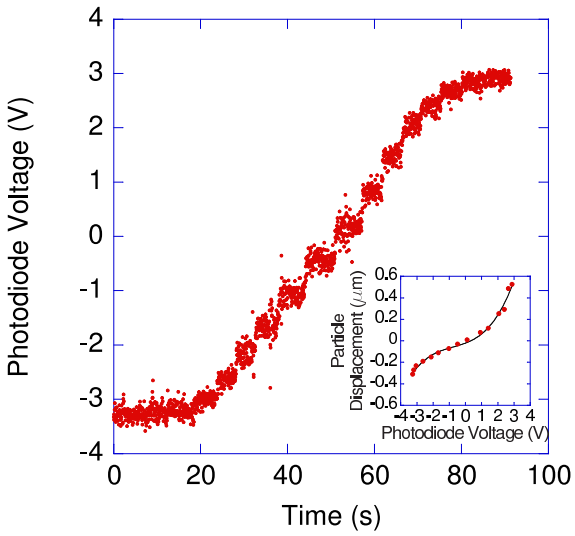

Figure 2.14: A graph of time vs the quadrant photodiode voltage. The duration of each step is not important provided enough points are obtained to calculate an average voltage. This average voltage (per step) is then related to the physical displacement of the quadrant photodiode, with each step corresponding to a 0.04 mm increment of the quadrant photodiode. Inset: The resulting quadrant photodiode position vs photodiode voltage graph, including a 3rd-order polynomial line of best fit.

2.5.3 Piezoelectric-stage Translations

The piezoelectric translators are calibrated so that they can be used in experiments requiring both static and dynamic positional control of the microscope stage. A standardised ruler with 10 μm increments is placed on the Optical Tweezers stage and a zero volt signal is applied to the piezoelectric translator. An image of the system is then recorded. A static calibration applies a constant DC voltage to a piezoelectric translator and allows the system to equilibrate before another image is taken. Dynamic calibrations constantly change the input voltage to the piezoelectric translator and continuously records images at 24 frames per second. The recorded images have an accuracy of ± 1 pixel or $\approx$ 175 nm with the 100$\times$ N.A. 1.3 lens. Figure 2.15 shows the results of a dynamic calibration. The relationship between applied voltage and stage displacement can then be generated.

A second method is employed to check the calibration when small voltages are applied to the system. This method uses a microscopic particle stuck on the bottom of the sample cell. A quadrant photodiode calibration is performed as in Section 2.5.2, and then a voltage is applied to the piezoelectric translator. The quadrant photodiode output is recorded and the displacement of the particle calculated. This

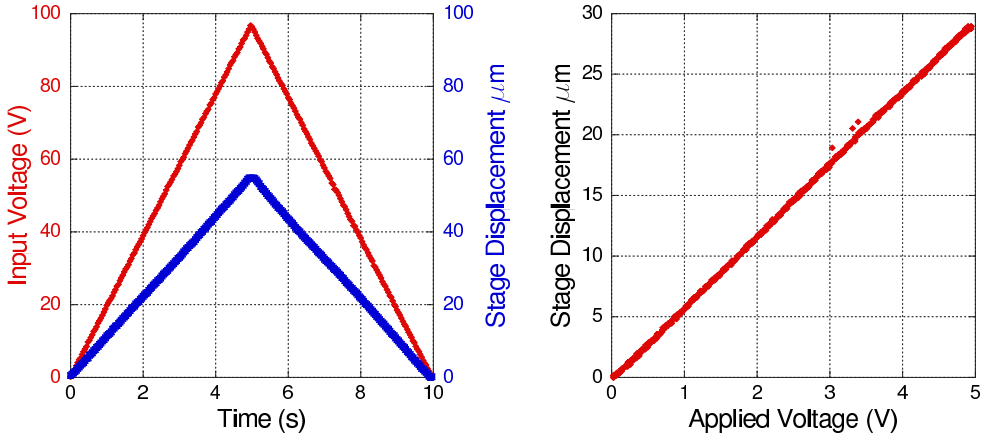

(a) (b)

Figure 2.15: Shown are two graphs used in the piezoelectric calibration. (a) The initial result showing the relationship between time and the signals collected. The triangular voltage used as an input (—) had an amplitude of 95 V with a frequency of 0.1 Hz. The corresponding stage displacement(—) has an amplitude of 57 μm and frequency of 0.1 Hz. (b) The resulting piezo displacement vs applied voltage curve. The line of best fit has a slope of 5.9359 μm/V.

calibration method is more accurate, but can only be applied to stage displacements of ± 3 μm. Translations larger than this move the image of the particle outside detection range of the quadrant photodiode.

2.5.4 Trap Strength Calibrations

These calibrations are carried out to determine the trapping force exerted by the laser upon the particle. There are several ways to calculate the optical trapping constant, k. The 3 most common methods to determine k are: equipartition, drag, and power spectral density (PSD) methods. Equipartition uses Brownian motion to relate the average position of a particle from the center of the optical trap to the thermal energy of the system. The equipartition method can only be used for low laser powers where particle fluctuations can be clearly resolved. At higher laser powers electronic noise can be comparable to position fluctuations greatly reducing the accuracy of the calibration. The stage is translated at a known veolcity, imposing a known fluid flow on a trapped particle, in the drag calibration. The displacement of the particle from the center of the trap is measured and the Stokes' drag force calculated. A Lorentzian is fitted to the power spectral density of the recorded particle displacements in the PSD calibration. To use either the drag or PSD method the viscosity of the solution must be known. Depending on how well the viscosity

is known, errors of $\approx 10\%$ can result. The details of each calibration method are described below.

The Equipartition Method

A particle is trapped in the Optical Tweezers at a low laser power. Using the DAQ and the quadrant photodiode the particle's position relative to the centre of the optical trap, r, is recorded as it fluctuates with Brownian motion. A sampling rate greater than 200 Hz is used and the position is monitored over several minutes. The average potential energy of the particle, $U = \frac{1}{2}k\langle \mathbf{r}\cdot\mathbf{r}\rangle$, is equal to the thermal energy, $\frac{1}{2}k_BT$ per degree of freedom. To ensure that the effects of an asymmetric trap are considered, the data is analysed along each axis separately to provide independent trap constants. The calibration performed solely along one axis therefore becomes

$$\begin{aligned} \frac{1}{2}k_x\langle r_x^2\rangle &= \frac{1}{2}k_BT \\ k_x &= \frac{k_BT}{\langle r_x^2\rangle}. \end{aligned} \tag{2.7}$$

The data set is split into N subsets, each of which yields a separate value for r_x^2. The standard deviation of these averages, $\sigma(r_x^2)$, is then calculated. Knowing that the error in k_BT is negligible in this experiment, then

$$\frac{\delta k_x}{k_x} = \frac{\delta(r_x^2)}{r_x^2},$$

where δk_x is the error in k_x, $\delta(r_x^2)$ is the error in r_x^2, and $\delta k_x = \sigma(r_x^2)/\sqrt{(N)}$. In all of the experimental results given, the error bars are calculated using $N = 100$.

The Drag Method

This calibration technique needs to be performed twice, along the x and y axis in the focal plane. The technique presented here assumes that all quantities act along this one axis. A particle is trapped in the Optical Tweezers at the desired laser power. The photodiode is positioned so the voltage signal is approximately centered around zero. A piezoelectric translator is supplied with a triangular signal causing the stage to translate at a constant velocity. The frequency of the triangular signal and its voltage range are used to determine the velocity of the stage using $V = 2f(V_H - V_L)\Delta$; where f is the triangular waves frequency, V_H is the maximum

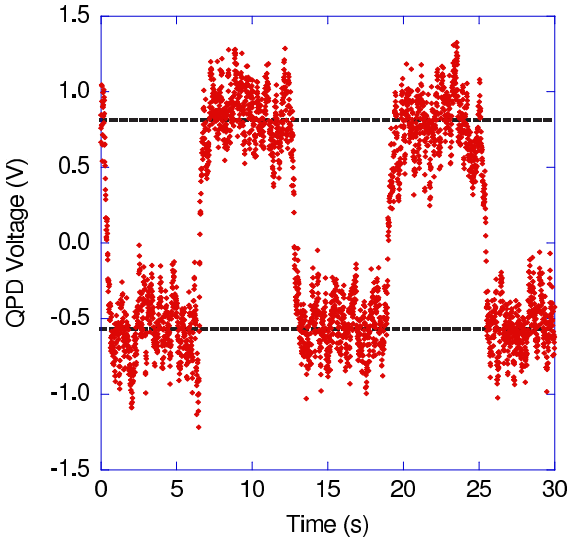

Figure 2.16: An example of photodiode voltage vs time that results from the particle moving away from the trap center during a drag calibration. The input triangular signal used to move the stage has a frequency of 0.08 Hz. Data was recorded at 200 Hz. The dashed lines represent the average voltage produced by the quadrant photodiode once the particle has reached a steady state. The scatter around this average value indicates there is a large error associated with this method.

triangular wave voltage, V_L is the minimum triangular wave voltage and Δ is the stage offset per volt (60μm/100V). Figure 2.16 shows the particle's position as the stage is translated, V_L and V_H correspond to the dotted lines. The drag force acting on the particle at a particular frequency is determined using Stoke's Law, $F = 6\pi\eta aV$, and is equal to the restoring force felt by the particle due to the optical trap in the steady state. Here η is the viscosity of the solvent and a is the hydrodynamic radius of the particle in the trap.

This procedure is repeated at several different frequencies. At each frequency, the average maximum and average minimum photodiode voltage is measured. Using the line of best fit calculated in Section 2.5.2 the maximum and minimum displacement, D_{Max} and D_{Min}, of the particle are calculated. The maximum displacement is caused by the drag force acting on the particle as it moves in one direction, the minimum drag force when it is moved in the opposite direction. The amount of data scattered above and below D_{Max} and D_{Min}, shown in Figure 2.16, indicates that there are substantial error margins using this technique.

By realising that the optical force and the Stokes drag force must be equal $F_{opt} = F_{drag}$, or $k \cdot r = F_{drag}$. Using this relationship it is possible to directly calculate the trapping constant k by plotting the values of "half-wave displacement"

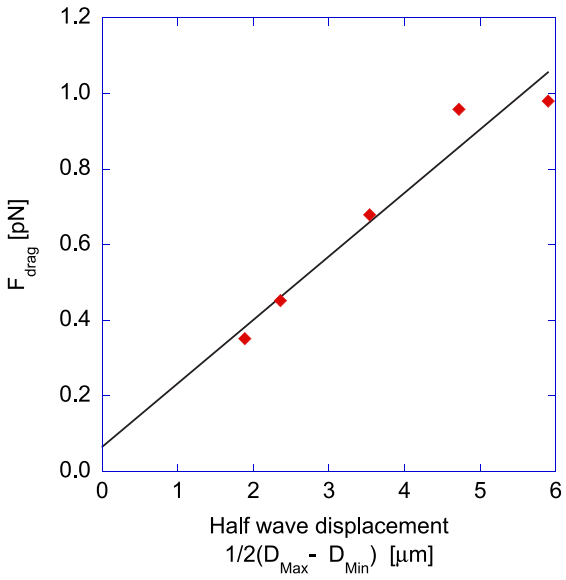

Figure 2.17: An example graph showing the drag force vs the displacement of the particle. The line of best fit is also plotted. The gradient of this best fit line is the optical trapping constant, k. Error bars of approximately 10% should be added to each data point.

as r, $r = \frac{1}{2}(D_{Max} - D_{Min})$, against F_{drag} as shown in Figure 2.17. The gradient of the line of best fit yields k.

The Power Spectral Density Method

This method can be used independently or in conjunction with the equipartition method. An excellent review on this method is provided by Sorensen *et al* [22]. A particle is trapped in the Optical Tweezers at a low laser power and using the DAQ and quadrant photodiode the particle's position is recorded. The PSD is calculated using the discrete fourier transform,

$$X(n) = \delta t \sum_{j=1}^{N} \exp\left(i2\pi f_j t_j\right) x(t_j), \tag{2.8}$$

where $x(t_j)$ is the particle's position recorded as discrete data, δt is the time interval between samples, $f_j = j/(N\delta t)$, $t_j = j\delta t$ and $X(n)$ is the Fourier transform of $x(t_j)$. The Power Spectral Density (PSD), P_n, is then calculated using

$$P_n = \frac{|X(n)^2|}{N\delta t}. \tag{2.9}$$

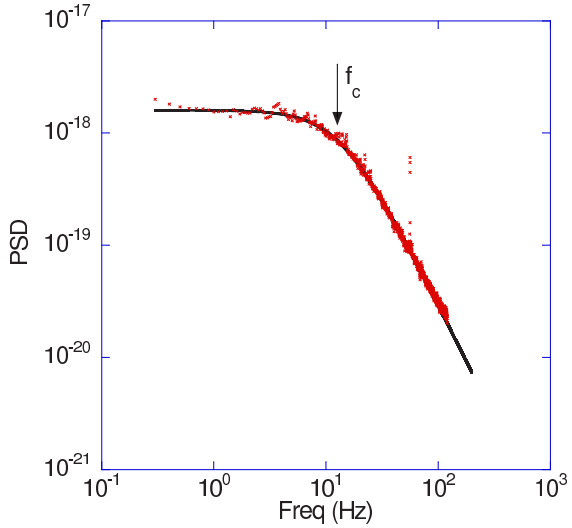

Figure 2.18: An example plot of the particle's displacement frequency vs its power spectral density. The fitting Lorentzian and f_c are also shown.

Following this the Lorentzian,

$$P_n = \frac{D}{2\pi^2(f_c^2 + f_n^2)}, \tag{2.10}$$

is fitted to the data. Here $D = k_B T/\xi$ is the diffusion constant, $\xi = 6\pi\eta a$ is the friction coefficient, η is the viscosity of the solution, a is the hydrodynamic radius of the particle in the optical trap, f_n is the frequency of sample n and f_c is a fitting parameter known as the corner frequency. By fitting f_c to the data, k is calculated using $k = 2\pi f_c \times 6\pi\eta a$. An example is shown in Figure 2.18.

Comparison of Calibration Methods

Each of the different calibration methods has its strengths and weaknesses. Large amounts of data can be recorded quickly and easily for equipartition, and a fast algorithm can yield an accurate trap constant almost immediately. However equipartition can only be used with weak optical traps. The PSD method can be limited by the fluid properties of the solution and the bandwidth of the position detection system (quadrant photodiode and circuit). Again large numbers of data can be obtained, although calculating the Fourier transform of large sets of data can be computationally expensive and take between a few seconds and several hours depending on the quantity of data collected. The accuracy of the Stokes' drag method depends upon the number of frequencies investigated, the fluid properties, and the

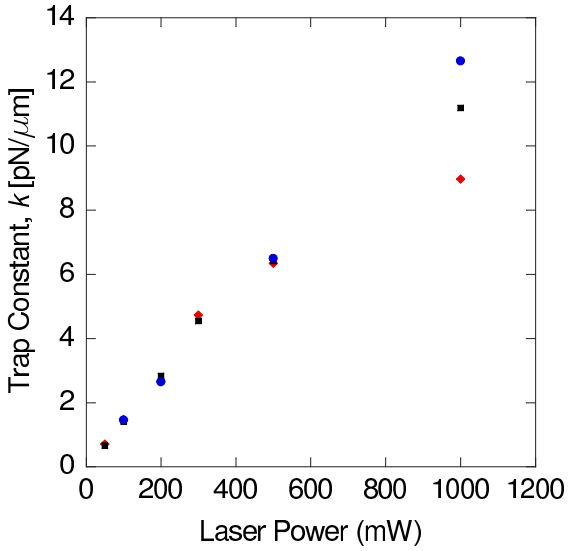

Figure 2.19: A graph showing trap constants determined using equipartition (●), drag (●), and PSD (●) constants as a function of laser power. At low laser powers the methods provide equivalent results. However at high laser powers equipartition is no longer able measure the particle's displacement with enough accuracy to provide the correct result.

hydrodynamic radius of the particle. The statistics are much poorer for Stokes' drag, that is only 10-20 data points are collected compared to 10,000 - 20,000 generated using equipartition or PSD. The choice of method to calibrate the optical trap clearly depends on the system to be investigated.

Figure 2.19 compares these three different calibration methods at various laser powers using the same particle. It can easily be seen that for low laser powers the equipartition method is equivalent to the Stokes drag and PSD methods. However this starts to fail at higher laser powers. Stokes drag and PSD both provide good results, although PSD has a much better set of statistics to sample from.

2.6 References

[1] J. C. Maxwell, *Theory of Heat* (1871).

[2] P. Lebedev, *Ann.Phys.(Leipzig)* **6**, 433 (1901).

[3] E. F. Nichols, G. F. Hull, *Phys. Rev.* **13**, 307 (1901).

[4] A. Ashkin, J. M. Dziedzic, *App.Phys.Lett.* **19**, 283 (1971).

[5] A. Ashkin, J. M. Dziedzic, *App.Phys.Lett.* **24**, 586 (1974).

[6] A. Ashkin, J. M. Dziedzic, *Science* **187**, 1073 (1975).

[7] A. Ashkin, *Phys. Rev. Lett.* **40**, 729 (1978).

[8] A. Ashkin, *Science* **210**, 1081 (1980).

[9] A. Ashkin, J. M. Dziedzic, J. E. Bjorkholm, S. Chu, *Opt.Lett.* **11**, 288 (1986).

[10] S. B. Smith, Y. Cui, C. Bustamante, *Science* **271**, 795 (1996).

[11] K. Sakata-Sogawa, M. Kurachi, K. Sogawa, Y. Fujii-Kuriyama, H. Tashiro, *Eur. Biophys. J.* **27**, 55 (1998).

[12] M. L. Bennink, O. D. Scharer, R. Kanaar, K. Sakata-Sogawa, J. M. Schins, J. S. Kanger, B. G. de Grooth, J. Greve, *Cytometry* **36**, 200 (1999).

[13] T. A. Nieminen, N. R. Heckenberg, H. Rubinstein-Dunlop, *J. Mod. Opt.* **48**, 405 (2001).

[14] A. I. Bishop, T. A. Nieminen, N. R. Heckenberg, H. Rubinstein-Dunlop, *Phys. Rev. A* **68**, 033802 (2003).

[15] K. Ladavac, D. G. Grier, *Optics Express* **12**, 1978 (2004).

[16] K. Ladavac, K. Kasza, D. G. Grier, *Phys. Rev. E* **70**, 010901 (2004).

[17] J. Leach, G. Sinclair, P. Jordan, J. Courtial, M. J. Padgett, *Optics Express* **12**, 220 (2004).

[18] P. Atkins, *Physical Chemistry 5th Ed.* (Oxford University Press, Melbourne, 1994).

[19] R. Eisberg, R. Resnick, *Quantum physics of atoms, molecules, solids, nuclei, and particles, 2nd Ed.* (John Wiley & Sons, 1985).

[20] S. Zumdahl, *Chemistry 3rd Ed.* (D.C. Heath and Company, Toronto, 1993).

[21] J. E. Molloy, M. J. Padgett, *Cont. Phys.* **43**, 241 (2002).

[22] K. Berg-Sorensen, H. Flyvbjerg, *Rev. Sci. Inst.* **75**, 594 (2004).